PAPER • OPEN ACCESS

Intermediate filaments ensure resiliency of single carcinoma cells, while active contractility of the actin cortex determines their invasive potential

New Journal of Physics
The open access journal at the forefront of physics

Deutsche Physikalische Gesellschaft DPG
IOP Institute of Physics

Published in partnership with: Deutsche Physikalische Gesellschaft and the Institute of Physics

OPEN ACCESS

RECEIVED
17 May 2021

REVISED
27 July 2021

ACCEPTED FOR PUBLICATION
28 July 2021

PUBLISHED
12 August 2021

PAPER

Intermediate filaments ensure resiliency of single carcinoma cells, while active contractility of the actin cortex determines their invasive potential

Carlotta Ficorella[1], Hannah Marie Eichholz[1], Federico Sala[2], Rebeca Martínez Vázquez[2], Roberto Osellame[2] and Josef A Käs[1,*]

[1] Peter Debye Institute for Soft Matter Physics, Leipzig University, Linnéstraße 5, 04103 Leipzig, Germany
[2] Istituto di Fotonica e Nanotecnologie (IFN)-CNR, Piazza Leonardo da Vinci 32, 20133 Milan, Italy
[*] Author to whom any correspondence should be addressed.

E-mail: jkaes@physik.uni-leipzig.de

Keywords: metastatic invasion, cancer cell migration in confinement, intermediate filament cytoskeleton, cortical contractility

Supplementary material for this article is available online

Abstract

During the epithelial-to-mesenchymal transition, the intracellular cytoskeleton undergoes severe reorganization which allows epithelial cells to transition into a motile mesenchymal phenotype. Among the different cytoskeletal elements, the intermediate filaments keratin (in epithelial cells) and vimentin (in mesenchymal cells) have been demonstrated to be useful and reliable histological markers. In this study, we assess the potential invasiveness of six human breast carcinoma cell lines and two mouse fibroblasts cells lines through single cell migration assays in confinement. We find that the keratin and vimentin networks behave mechanically the same when cells crawl through narrow channels and that vimentin protein expression does not strongly correlate to single cells invasiveness. Instead, we find that what determines successful migration through confining spaces is the ability of cells to mechanically switch from a substrate-dependent stress fibers based contractility to a substrate-independent cortical contractility, which is not linked to their tumor phenotype.

Abbreviations used in this paper

CK-	cytokeratin
ECM-	extracellular matrix
EGF-	epithelial growth factor
EMT-	epithelial to mesenchymal transition
IF-	intermediate filaments
MF-	microfilament
MT-	microtubule
OS-	optical stretcher
WT-	wild type

1. Introduction

Breast carcinoma is the most common invasive neoplasia diagnosed in women worldwide, with the majority of deaths being a consequence of invasion of the surrounding tissue and metastasis (Wullkopf *et al* 2018). Metastasis originated from carcinomas are the product of a developmental process based on a complex succession of biological occurrences, whereby epithelial cells in primary tumors infiltrate the local extra-cellular matrix (ECM) and stroma layers, intravasate into the blood vessels, arrest at distant organs when surviving the transport through the vasculature, penetrate the parenchyma of the new site tissues and resume proliferating, hence, generating new neoplastic masses. At a molecular level, primary tumors with

invasive properties are characterized by a loss of epithelial characteristics, combined with a gain in mesenchymal ones, a process that closely resembles the epithelial-to-mesenchymal transition (EMT) occurring in embryonic development (Kalluri and Weinberg 2009, Ribatti *et al* 2020). This leads to reduction of intracellular adhesion, often caused by a loss of E-cadherin, and changes in cellular plasticity resulting from morphological and phenotypical conversions (Chiang and Massagué 2008, Ilina *et al* 2020, Lange and Fabry 2013, Mierke 2015).

During cancer related EMT, epithelial cells detach and reorganize by switching to a mesenchymal progenitor-cell phenotype, causing an up-regulation of the mesenchymal markers such as N-cadherin and vimentin. The expression of N-cadherin, in particular, leads to the rearrangement of the cytoskeleton and to the detachment of the cells from the epithelial cluster, thus increasing their motility and allowing them to migrate as single cells. The genetic instability of tumor cells facilitates mutation and gene translocation events, resulting in the activation of some genes and oncogenes that lead to the expression of the malignant phenotype (Ribatti *et al* 2020).

Vimentin protein expression is traditionally associated with high tumor risk and chemoresistance. This has been supported by the fact that vimentin is the major cytoskeletal component of, and is consistently expressed and conserved in, mesenchymal cells (Danielsson *et al* 2018, Kokkinos *et al* 2007, Mendez *et al* 2010, Raymond and Leong 1989). The argument that vimentin expression mainly occurs in those cell types displaying invasive phenotypes reinforces the hypothesis that vimentin is related to high invasive abilities. Vimentin filaments assemble into a flexible fibrous matrix that surrounds the nucleus and attaches to the endoplasmatic reticulum and mitochondria, and extends within the cell interior up to the membrane, allowing the cell to respond to mechanical stresses (Gardel *et al* 2008, Hu *et al* 2019, Patteson *et al* 2019). Vimentin is expressed together with CKs in many normal and neoplastic endocrine cell types (Hendrix *et al* 1997, Polioudaki *et al* 2015). As it is known for being involved in tumor initiation and development, including cancer related EMT, vimentin has gained clinical significance as tumor marker, and antibodies targeting vimentin are also employed as markers in histopathological diagnosis, in order to distinguish epithelial and mesenchymal tumors, such as malignant melanomas and lymphomas (Danielsson *et al* 2018).

CKs belong to the largest group of IFs, and show a remarkable degree of molecular diversity. Twenty distinct CK isotypes, with molecular weights ranging from 40 to 68 kDa, have been so far identified in human epithelia, with CK1-CK8 being type II basic epithelial proteins, and CK9-CK20 being type I acidic epithelial proteins. In cells, type I keratins pair with type II keratins to form heterodimers that interact with each in other to form flexible and stable filaments. Keratin filaments constitute a fibrous dynamic network that extends from the nucleus to the plasma membrane, and enables cells to resist mechanical stress, thus providing strength and elasticity (Moll *et al* 2008). As pairs of basic and acidic CKs are expressed in different ways in epithelial human cells at distinct stages of differentiation and development, CKs are useful for pathologists to identify epithelial (cytokeratin positive) cells versus non-epithelial (usually cytokeratin negative) tumors. CKs are expressed among different breast cancer cell lines and are down-regulated during metastatic invasion and progression, and such regulation of keratin in epithelial tumor cells is viewed as one of the key mechanisms behind EMT (Karantza 2011, Seltmann *et al* 2013, Shao *et al* 2012).

Importantly, the ability to co-express both keratin and vimentin IFs in cells was shown to confer migratory ability to single cells in cancers such as malignant breast carcinoma (Domagala *et al* 1990, Hendrix *et al* 1997, Raymond and Leong 1989, Thompson *et al* 1992), whereas inducing vimentin expression in vimentin negative epithelial cells was shown to affect cell–cell adhesions by disrupting keratin-desmosome interactions (Mendez *et al* 2010).

The question that we attempt to address in this study is whether a difference can be drawn between the expression of specific protein markers (identifying the EMT status of a cell) and the real contribution of such proteins to the EMT process. This study examines the significance of vimentin and keratin protein expression in six breast carcinoma cell lines during migration through a constricting rigid environment, in order to refine the characterization of their EMT status and compare how the expression of specific IFs relates to the standard assumptions of the EMT model. Two fibroblast cell lines derived from mouse embryo are also included in our model, as mechanically they well represent an advanced EMT stage. We simulate the process cancer cells undergo during migration through the extracellular matrix (ECM) and extravasation, with migration assays performed on chips equipped with three dimensional rigid micro-constrictions (for more details, see Ficorella *et al* 2019 and Sala *et al* 2021). We initially focus on the response of the IF cytoskeleton to the compressive stress applied by the narrowing micro-constrictions, and we observe to what extent does the IF cytoskeleton contribute to individual cancer cell migration into narrow spaces. We find that there is no noticeable difference in the behavior of the keratin and vimentin networks during migration through our micro-constrictions, and that vimentin IF expression does not always correlate with the invasive behavior exhibited by the different cell lines in the micro-channel assay.

Since EMT is also characterized by an increase in cellular contractility (Kraning-Rush *et al* 2012, Mierke *et al* 2008), these findings prompted us to investigate the role of contractility in confined migration. Cellular contractility has been object of intense study since it is known to be a key mechanism not only in cell motility and tissue formation, but also in invasion. Contractility can be fostered by two distinct cell mechanisms: actin stress fibers, which generate force dipoles when cells navigate through the ECM (Gardel *et al* 2010, Mierke *et al* 2008), and the acto-myosin cell cortex, which gives rise to isotropic contractions (Chugh and Paluch 2018, Gyger *et al* 2014, Murrell *et al* 2015, Salbreux *et al* 2012). In a previous study, we observed in details how the actin cytoskeleton is impacted under conditions of strong confinement, and found that activation of actin stress fibers contractility was a requirement for depolymerization of the actin cytoskeleton and successful migration through the micro-funnels (Ficorella *et al* 2019). Here, we focus on the second type of contractility, and show how the acto-myosin cortex is a major component for invasiveness through the narrow spatial confinement. We propose the idea that the ability to easily switch between distinct contractility mechanisms is what primarily allows individual cells to navigate through interstitial spaces and survive large deformation stresses.

2. Methods and materials

2.1. Cell culture

The human breast cancer cell lines used in this study were purchased by ATCC. MCF-10A cells (non-tumorigenic epithelial) were cultured in 1:1 mixture of Dulbecco's Modified Eagle's Medium (DMEM) and Ham's F12 medium (Biochrom, with L-Glutamine) supplemented with 5% Horse Serum (HS), 20 ng ml^{-1} epidermal growth factor (EGF), 10 μg ml^{-1} Insulin (Sigma-Aldrich), 100 ng ml^{-1} Cholera Toxin (Sigma-Aldrich), 500 ng ml^{-1} Hydrocortisone (Sigma-Aldrich), and 1% 10 000 U/ml penicillin/streptomycin (Biochrom). The EGF-free MCF-10A cells were cultured under the same conditions, except for the lack of EGF in the medium. MCF-7 cells (cancerous epithelial, derived from adenocarcinoma) were cultured in Eagle's minimal essential medium (Sigma Aldrich) supplemented with 10% fetal calf serum, 10 μg ml^{-1} Insulin (Sigma-Aldrich), 100 mg ml^{-1} sodium pyruvate 100 mM (100X) (Life Technologies), 1% non-essential amino acids (100X) (Life Technologies), and 1% 10 000 U/ml penicillin/streptomycin (Biochrom). MDA-MB-231 (mesenchymal, highly aggressive and derived from adenocarcinoma) and MDA-MB-436 cells (mesenchymal, derived from metastatic site) were cultured in DMEM (Biochrom, with 4500 mg l^{-1} glucose, L-glutamine, without sodium pyruvate) supplemented with 10% fetal calf serum FCS (Biochrom) and 1% 10 000 U/ml penicillin/streptomycin (Biochrom). MDA-MB-468 cells (mesenchymal, derived from pleural effusion of adenocarcinoma) were cultured in RPMI 1640 medium (Capricorn Scientific) supplemented with 10% fetal calf serum FCS (Biochrom), and 1% 10 000 U/ml penicillin/streptomycin (Biochrom).

3T3 NIH Swiss mouse fibroblasts, derived from mouse embryos, and the vimentin-negative mouse fibroblasts, derived from vimentin free mouse embryos, were kindly provided by the Magin Lab (Division of Cell & Developmental Biology, Institute of Biology at the University of Leipzig) and cultured in DMEM supplemented with 10% FCS and 1 mM sodium pyruvate. The cells were cultured at least twice per week at 80% confluence or less (care was taken to not allow the cells to become confluent).

2.2. Cell immunostaining

Commercially available monoclonal and polyclonal antibodies were selected for the detection of keratin and vimentin IF in paraffin-embedded and methanol-fixed human breast cancer cell lines. The tested primary antibodies were the following: anti-pan cytokeratin AB_780038 (rabbit, polyclonal, targeting CK4, CK5, CK6 and to a minor extent CK8, CK14 and CK16), anti-cytokeratin 8/18 AB_10986863 (mouse, cocktail), and anti-vimentin AB_2216267 (chicken, polyclonal). As secondary antibodies, the donkey anti-rabbit IgG (H + L) highly cross-adsorbed AB_2216267 (Alexa Fluor 488), the goat anti-mouse IgG (H + L) highly cross-adsorbed AB_2534088 (Alexa Fluor 488), and the goat anti-chicken IgY (H + L) cross-adsorbed AB_2535756 (Alexa Fluor 633) were used. Hoechst-34580 was also used to label the nuclei. The tumor cells observed in this study were fixed in methanol for keratin and vimentin immunostaining. The primary antibodies were incubated on the cells for one hour at room temperature. The optimal dilution for each primary and secondary antibody allows a strong specific protein labeling with minimal non-specific background labeling, and was determined after several trials.

2.3. Experimental procedure of migration assays and cell imaging

The migration assays were performed on chips containing polymeric narrowing micro-constrictions with a final width ranging between 3 to 7 μm, and a top-bottom distance of 10 μm. The final cross-sectional area of the funnel was significantly smaller than the cell cross sectional area (supplemental figure 2

(https://stacks.iop.org/NJP/23/083028/mmedia)). Cells were seeded on the culture chamber of the micro-constriction chips at a density of 10^6 cells ml^{-1}. The density was assessed with an EVE cell counter. A mixture of medium and chemoattractant (1 μl ml^{-1}) was pipetted into the collecting chamber in order to allow directional cell migration toward the row of micro-constrictions. EGF was most commonly used as chemoattractant, although glucose and sodium pyruvate were equally successful. For the phase contrast long term observations, the chips were placed in a 12-well plate with plastic bottom (CELLSTAR, Greiner Bio-One). More details about the chip fabrication procedure can be found in Sala *et al* (Sala *et al* 2021). In particular, we highlight that the specific design of these chips enables high-quality and high-magnification imaging of the migrating cells, while allowing an exquisite control on the shape and size of the micro-constrictions. The cells were observed for four days, the medium was refilled every 12 h. Time-lapse phase contrast recordings were acquired with 10X EC Plan-Neofluar M27 objective (NA 0.25, air) using a Zeiss Axio Observer Z1 and selecting a 300 s interval between acquisitions. The microscope was equipped with an on-stage incubation chamber which maintained the temperature at 37 °C and CO_2 concentration at 5%. The Zeiss Axio Observer Z1, equipped with a Yokogawa CSU-X1A5000 spinning disk confocal scanning unit was also used to acquire fluorescence images of the intermediate filaments and nuclei upon cell fixation, with a 100X Plan-Apochromat M27 objective (NA 1.4, oil). Images were acquired with a Hamamatsu Orca Flash 4.0 camera. Gamma values were corrected to obtain high contrast images.

2.4. Western blots

CK5, CK6a/CK6b, CK8, as well as vimentin were targeted. The antibodies employed were kindly donated by the Magin Lab (Division of Cell & Developmental Biology, Institute of Biology at the University of Leipzig) and have been extensively validated by previous independent western blot assays. The primary antibodies were the following: anti-vimentin (rabbit, 1:8000), anti-CK5 L55 (rabbit, 1:2500), anti-CK6a/CK6b L27 (rabbit, 1:10 000), anti-CK8 L13 (mouse monoclonal, 1:1000), and anti-CK19 L276 Troma III (rat, 1:50). The typical amount of lysate loaded per pocket on the SDS-page gel ranged between 8 and 12 μl for the epithelial cell lysates, or between 12 and 15 μl for the mesenchymal cell lysates. After electrophoresis, the proteins in the polyacrylamide gel were immediately transferred on a nitrocellulose membrane via semi-dry blotting. Overnight incubation with Coomassie R250 on a separate gel was performed beforehand as control, to confirm that the protein load in the gel upon electrophoresis was indeed correct. Following the blotting, the membrane was stained with PonceauS, to ascertain the quality of the protein transfer in each lane, and later incubated with the selected antibodies.

2.5. Optical stretcher measurements and quantification of contractility

The optical stretcher (OS) is a laser-based optical trap, which is used for contact-free trapping and deforming (stretching) micrometer-sized soft matter particles, such as biological cells in suspension. The viscoelastic properties of individual cells in suspended state are examined in their ground state, without any adhesion effects due to the contact with other cells or with the measurement device itself (Guck *et al* 2001, 2005, Gyger *et al* 2014). The cells to be examined are located in a flow channel and pumped with a microfluidic pump (Fluigent). They are successively captured and held between two opposing divergent laser beams (Fibolux Fibotec, with $\lambda = 1064$ nm) of Gaussian profile with a trap power of $P_{\text{trap}} = 100$ mW. The laser power was then increased to $P_{\text{stretch}} = 800$ mW for 5 s, inducing an optical stress of $\sigma \approx 0.8$ Pa. This steady increase in laser power caused the force acting on the cell surface to increase and the cell to be deformed along the laser axis. After 5 s, the laser power was turned back to the initial 100 mW. The deformation of the cell is measured by video microscopy (Guck *et al* 2005). In general, the magnitude of the deformation is a function of time, due to the viscoelastic properties of the cells. By analyzing the major and minor axis of the cell in the trapping and stretching phase, conclusions can be drawn about the deformation. It is also possible to make statements about the size distribution of the measured cells. Attention was paid to measure as many cells as possible (about at least 1000 cells), in order to obtain an accurate broad distribution of the deformation of each cell line. No drugs or dyes were added. The median values of the contractility were determined upon completion of the OS measurements through a mathematical model based on the active Kelvin–Voigt model.

3. Results

Molecular classification does not necessarily correlate to the ability of cells to actively migrate through confining spaces.

The device used to test the potential invasiveness of the six breast carcinoma cell lines was designed to include two millimeter-sized reservoirs, separated by a 'migration region' containing many aligned funnel-shaped micro-constrictions. These were built by using an SU-8 3025 resin, an epoxy-based negative

Table 1. Migration assay results.

Cell type	Molecular classification	Invasiveness in microconstrictions	Actin stress fibers formation
MCF-10A (EGF-free)	Ba	Only leading cells	No
MCF-10A	Ba	Passed through	Yes
MCF-7	LA	No	No
MDA-MB-468	TNA	Passed through	Yes
MDA-MB-436	TNA	No	No
MDA-MB-231	TNB	Passed through	Yes
MF Vim −/−	Fibroblasts	Passed through	Yes
MF Vim +/+	Fibroblasts	Passed through	Yes

photoresist used in photo lithography. One of the reservoirs was dedicated to cell growth (culture chamber). The second reservoir, filled with cell medium and with a chemoattractant to stimulate directional migration, collected the cells that successfully migrated through the constrictions in the migration region. Each reservoir can contain 35 μl of medium, which ensures the experiments to be carried out up to 12 h before complete evaporation. The micro-constrictions have a minimum aperture ranging between 5 to 10 μm. The distance between the top and the bottom layer (constriction height) is 10 μm. This allowed cells and their nuclei to be compressed in all three spatial dimensions. Forcing cell migration in the narrowing 3D glass-like constrictions offered the advantage of observing how physical confinement alters cellular behavior and morphology, without the involvement of ECM proteases and other regulatory enzymes and growth factors.

In Ficorella *et al* (2019), we showed that fundamentally different cell types can display the same invasive potential in spatial confinement. Both the highly aggressive mesenchymal MDA-MB-231 and the normal epithelial MCF-10A cells had exhibited speed and directionality of motion upon stimulation with the chemoattractant, and had successfully achieved migration through the narrow constrictions. High resolution immunofluorescent imaging had revealed that when moving in the culture chamber and entering the micro-funnels, motile cells displayed aligned actin stress fibers and a cortical actin shell in proximity of the membrane. We showed how squeezing through the micro-funnel aperture necessitates actin fiber depolymerization, cortical cytoskeleton disruption and deformation of cell membrane. The MDA-MB-231 cells assumed a motility mode that strongly resembled blebbing while squeezing through the micro-funnels. In the strongly adherent and polarized MCF-10A cells, the actin remodeling occurred by following the same pattern as the mesenchymal cells, except for the formation of actin rich lamellipodial protrusion at the cell leading edge during the squeezing phase, necessary to generate sufficient force for translocation of the cell body through the constriction opening. We also showed that the metastatic mesenchymal MDA-MB-436 cells did not exhibited migratory behavior and showed no formation of directional actin bundles as in the case of the MDA-MB-231 and the MCF-10A cells (supplemental figure 1). This ultimately revealed how critical actin stress fibers formation is for the actin cytoskeleton depolymerization and successful migration in rigid confinement (Ficorella *et al* 2019).

In this study, we introduced more cell lines with the intention of drawing more general conclusions about the migration behavior of single breast carcinoma cells in our microstructures. The following cell lines were selected: MCF-10A cells grown in medium not supplemented with epithelial growth factor (EGF) (20 g l^{-1}), the cancerous epithelial MCF-7, and the cancerous mesenchymal MDA-MB-468. The vimentin-positive and the vimentin-negative 3T3 NIH Swiss mouse fibroblast cells have also been included as a prototype for mesenchymal cells at an advanced EMT stage.

The EGF-free MCF-10A cells have shown noticeable differences when compared to the original MCF-10A cells, both in size and motility behavior (supplemental figures 2(a) and (b)). EGF and EGF receptor are well-known for playing a crucial role in wound healing by stimulating proliferation of epithelial cells and fibroblasts for dermal and epidermal regeneration (Bodnar 2013, Wong and Guillaud 2004). After three months of EGF-free culture, the MCF-10A cells showed a rounder morphology, smaller size, while growing at a slower proliferation rate and in compact clusters. In the microchips, they grew in a compact monolayer with little to no presence of lamellipodial protrusions, but only the leading cells in the monolayer were successfully pushed through the funnels. The slow but successful migration of the leading cells was followed by the arrest of the monolayer advancement and cell proliferation (supplemental figure 3). On the other hand, the epithelial cancerous MCF-7 cell line was not responsive to any of the employed chemoattractants, and showed no motile behavior (supplemental figure 3). Similar to the MDA-MB-436 cell line, the MDA-MB-468 was extracted from pleural effusion of mammary gland and other breast tissues. However, contrary to the MDA-MB-436 cells, they successfully navigated through the micro-constrictions with a seemingly bleb-like motility mode, maintaining a roundish, ameboid

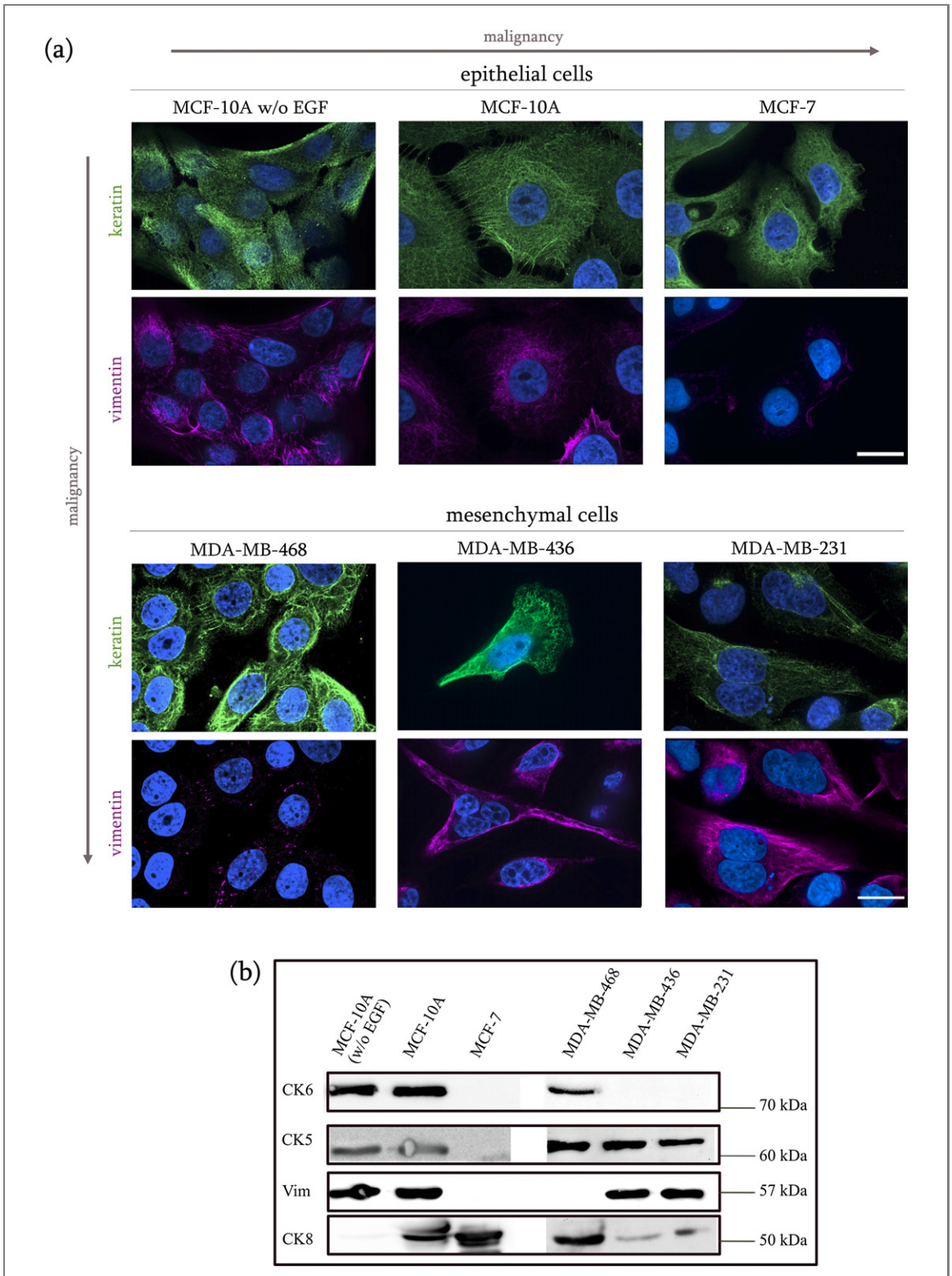

Figure 1. Cytokeratin and vimentin expression in breast cancer cell lines. (a) Methanol cell fixation was performed on the selected epithelial and mesenchymal cells to visualize keratin and vimentin filament distribution, with polyclonal and monoclonal antibodies respectively. Keratin filaments are shown in green, vimentin filaments in violet. The nuclei (blue) were stained with Hoechst-34580. The CK8/18 cocktail successfully stained the keratin filament in all cell types. The pan-cytokeratin antibody did not provide a fluorescent signal for the MDA-MB-436. While the keratin IFs appear to be densely and homogeneously distributed within the two MCF-10A cell types and the mesenchymal cells, in the epithelial MCF-7 cells they are mainly concentrated at the boundaries of the tight cell clusters. Immunostaining has confirmed the absence of vimentin expression in the MCF-7 and MDA-MB-468 cell lines. Scale bar is 20 μm for all panels. (b) Anti-keratin 5, 6(a & b), 8, and anti-vimentin western blots for the epithelial cells are shown. In spite of the low intensity signal for the CK5 blot, two bands can be observed at an approximate molecular weight of 60 kDa for the MCF-10A cell types. In accordance to their molecular classification, the MCF-7 cells turned negative for the basal CK5/6, and positive for the luminal CK8. While the wild type MCF-10A cells were positive for all three keratin types, the EGF-free cells resulted positive for CK5/6, but not for CK8. The mesenchymal lines were positive to CK5 and CK8, but only the MDA-MB-468 were positive to CK6.

morphology, strongly resembling the MDA-MB-231 cells (supplemental video 1). Finally, both the vimentin-positive and the vimentin-negative 3T3 mouse fibroblasts equally achieved migration through the micro-constrictions (data shown in supplemental videos 2 and 3).

Table 1 offers a summary of the migration results, with the cells listed in order of aggressiveness on the EMT scale and classified into basal (Ba), luminal A (LA), triple negative A (TNA), and triple negative B (TNB) subtypes, according to available literature.

Intermediate filament expression determines the EMT status of mammalian cells, but not their ability to navigate through confinement.

After observing the heterogeneous migratory response of our cell lines in the micro-constriction chips, we decided to investigate the IF expression for each cell type and see whether or not it correlates to their ability to navigate through the constrictions. PanCK, CK8/18, and vimentin antibodies were used for immunofluorescence labeling in order to visualize the IF expression in our six breast cancer cell lines (figure 1(a)). As expected, all cell lines showed positive staining for CK8/18. The mesenchymal MDA-MB-231 and both the epithelial MCF-10A cell types constitutively co-express vimentin and keratin. Dual immunofluorescence labeling revealed remarkably dense keratin and vimentin networks, particularly in the MCF-10A cell line. The vimentin filament network in the EGF-free MCF-10A cells appears visibly less dense than in the original MCF-10A cells, suggesting that a downregulation of vimentin has occurred. Vimentin was not detected in the cancerous epithelial MCF-7 cells, nor in the cancerous mesenchymal MDA-MB-468 cells. Interestingly, while the CK8/18 antibody cocktail worked for all cell types, the anti-pan cytokeratin antibody targeting CK5 and CK6 failed to detect filaments in the mesenchymal MDA-MB-436 cells, suggesting that this cell type may be characterized by a less heterogeneous keratin protein expression. Importantly for this specific cell type, the inability of displaying an invasive migratory behavior despite their being a triple negative, vimentin-positive, mesenchymal line, could be correlated to the expression of luminal keratins such as CK8 and CK18 and a lack of expression of basal keratin such as CK5 and CK6. To validate this assumption and ascertain more accurately the IF content in our cell lines, we performed western blots, specifically targeting vimentin and a group of keratins commonly expressed in adenocarcinomas (and partly in the immunofluorescence assays), namely CK5, CK6a/CK6b, and CK8 (figure 1(b)).

The expression of high molecular weight CK5 (and its type I acidic partner CK14) in breast tissue defines the carcinoma as basal-like, and is associated with poor prognosis and poor survival chances (Karantza 2011, Shao *et al* 2012). CK5 was detected, as expected, in all triple negative mesenchymal cell lines and in both basal MCF-10A cell types, but not in the luminal MCF-7. Presence of CK5 was confirmed in the MDA-MB-436 cells, where the pan cytokeratin solution containing anti-CK5 antibodies failed to show any filamentous structure. It is important to notice that the immunostaining assays were performed for multiple cell lines at the same time. However, the fact that the CK5 blot provides such a clear result likely suggests that during the pan cytokeratin immunostaining in the MDA-MB-436 cells not enough primary antibody bounded to the protein of interest, which caused the secondary antibody to fail to detect CK5 filaments.

CK6a and CK6b isoforms are present in stratified epithelial and their overexpression is associated to abnormal differentiation and enhanced cell proliferation rate during wound healing, as well as in diseases, such as actinic keratosis, psoriasis, and cancer. When used as epithelial marker, CK6 is often used together with CK5. CK5/6 expression entails a basal-like molecular phenotype, which is associated to poor prognosis and in the breast it can be used to distinguish between ductal hyperplasia (CK5/6-positive) and solid papillary carcinoma (CK5/6-negative) (Moriya *et al* 2009). Interestingly, CK6a/6b was detected in both MCF-10A types and in the cancerous MDA-MB-468 cells, but not in the invasive MDA-MB-231 cells.

The simple epithelial keratins CK8 is expressed in most adenocarcinomas. The pair CK8/18 is known to ensure a flexible intracellular scaffolding that can resist external forces, thus maintaining cellular integrity, as well as mitochondrial structures. Importantly, besides its role of structural support, CK8 is also known to modulate intracellular signaling, thus affecting pathologies such as liver disease (Ku *et al* 2010) and carcinogenesis, through a number of signaling pathways involved in cell growth, motility and apoptosis (Weng *et al* 2012). As downregulation of CK18 in metastatic breast cancer has been recognized by gene profiling, this cytokeratin is widely used as a reliable epithelial marker in diagnostic histopathology (Karantza 2011). Here, the luminal marker CK8 was easily detected in the MCF-10A and in the MCF-7 cells, as well as in the mesenchymal cell lines. The weak bands that are visible on the MDA-MB-436 and MDA-MB-231 lanes may signify that this specific cytokeratin is also expressed in these cell lines, perhaps to a minor extent. The EGF-free MCF-10A cells show no expression of CK8. Because the MCF-10A cell line possesses the ability to express both basal and luminal markers, despite being characterized by a basal-like phenotype (Qu *et al* 2015), the downregulation of CK8 expression in the EGF-free type may indicate a

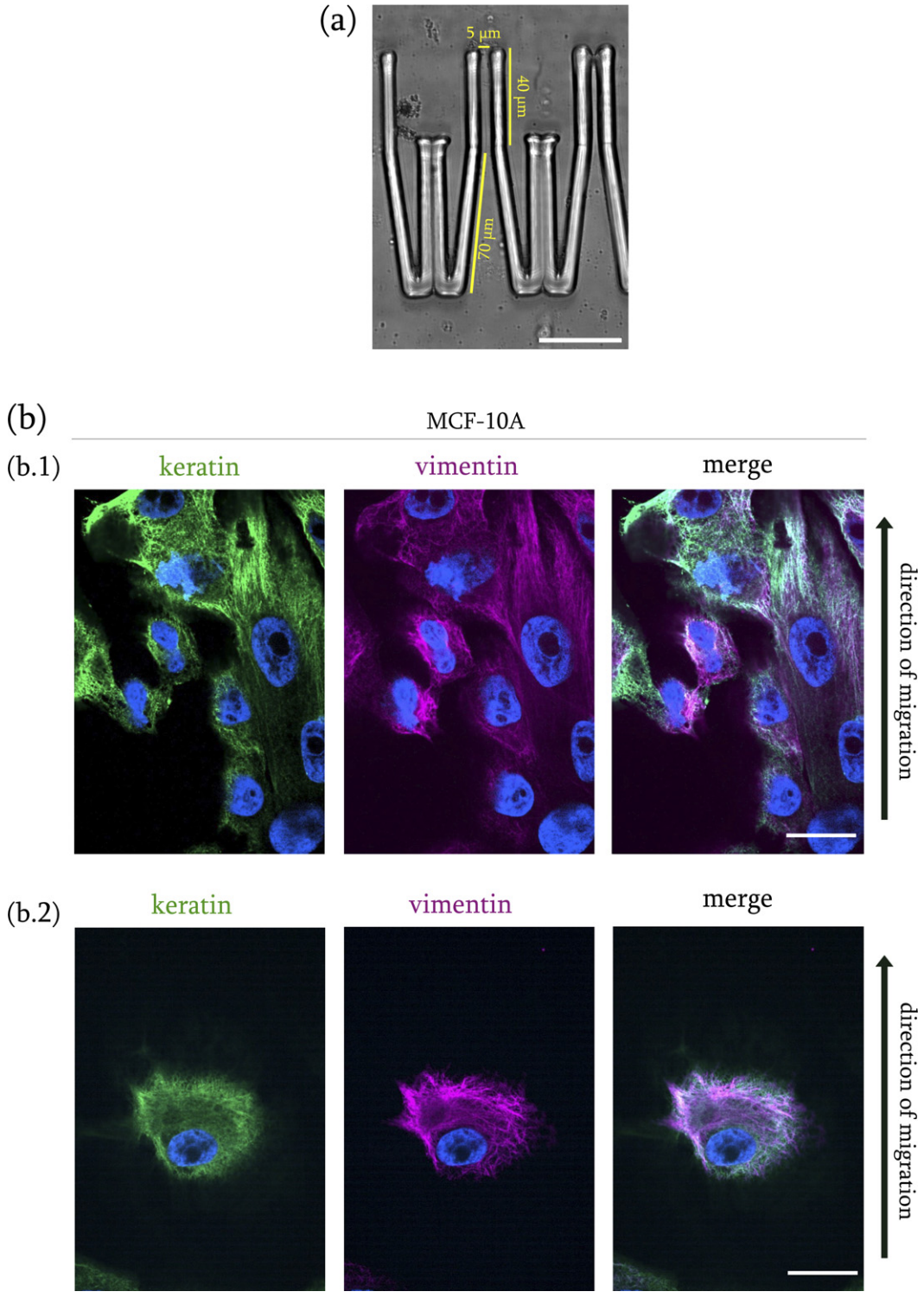

Figure 2. IF single cell migration through narrow microconstrictions. (a) Phase contrast image of the funnel + channel constriction. Scale bar is 40 μm. (b) MCF-10A cells after squeezing through the narrow channel. (b.1) The vimentin and keratin networks, as well as the cell nuclei, temporarily retain an elongated configuration due to the squeezing process through the narrow channel. (b.2) MCF-10A cell after migration through the channel. Here we can see that the dense vimentin and keratin networks have reacquired the typical configuration, homogeneously spreading from the nucleus to the membrane. Scale bar is 20 μm for all panels.

progressive loss of luminal features when these cells are not exposed to EGF expression, and therefore a consolidation of their basal origin.

3.1. Intermediate filaments in living cells organize in bundles when undergoing compression

To gain some insight on the response of keratin and vimentin networks in living cells to compressive stress, we closely observed their re-arrangement after migration through the micro-funnels. For this purpose, we

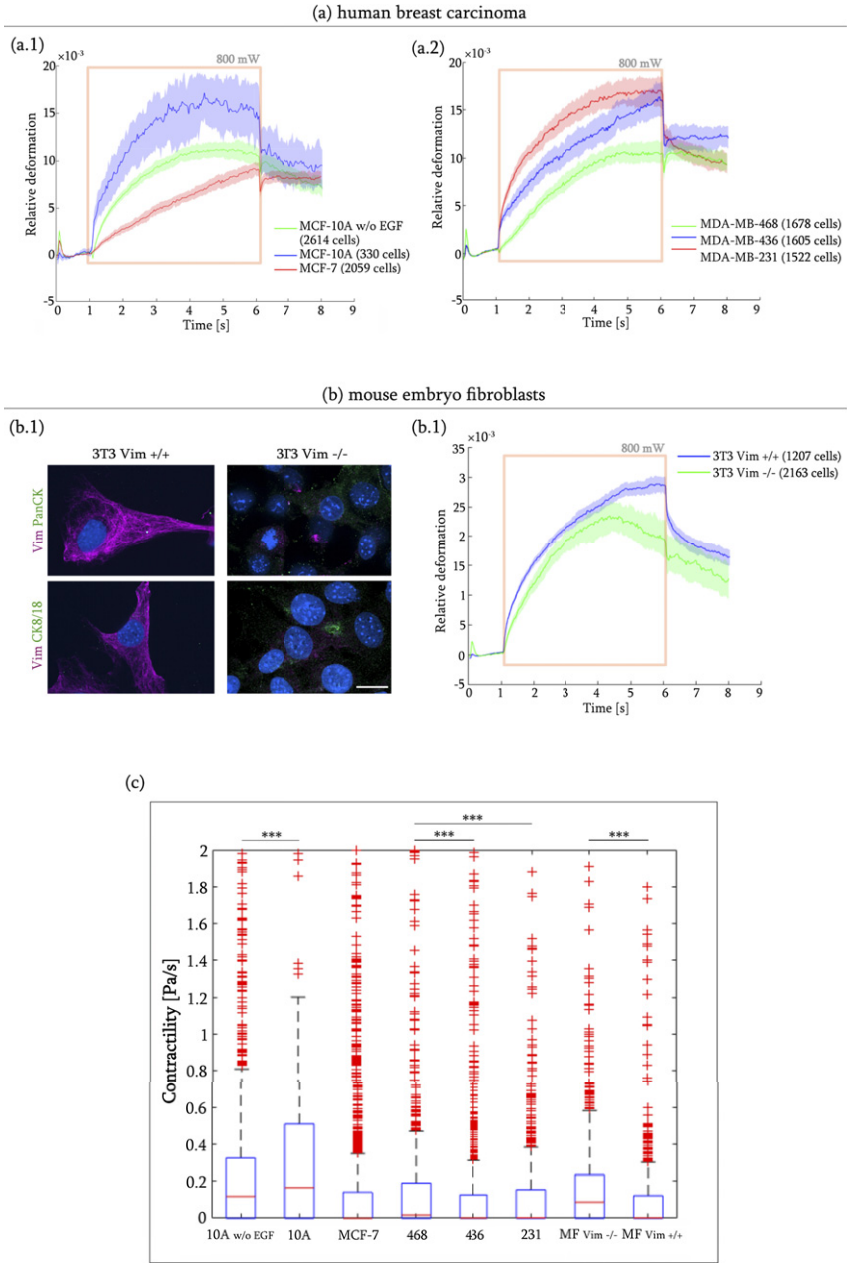

Figure 3. Optical deformability curves of mammalian carcinoma cell lines and mouse fibroblast cell lines. (a.1) Relative mean deformation of the epithelial EGF-free MCF-10A cells (in green), MCF-10A (in blue) and MCF-7 (in red) cells is plotted. $T = 0-1$ s indicates the trapping stage, where the laser power is used only to trap and stabilize single cells, without stretching them. During the stretching stage $t = 1-6$ s the laser power increases stepwise up to 800 mW (orange rectangle). The epithelial cell type MCF-10A and MCF-10A w/o EGF show an increasing contractile behavior, during stretch, whereas the MCF-7 deformation curve shows a drastically reduced contractility. (a.2) Relative mean deformation of the mesenchymal MDA-MB-468 (in green), MDA-MB-436 (in blue), and MDA-MB-231 (in red) cells. Overall, the mesenchymal cells are much less contractile than the epithelial cells when optical stress is applied. The MDA-MB-436 cell line complies to a passive viscoelastic response without active contraction, while the other two deformation curves show mesenchymal cells with a contractile behavior. The light colored bands superimposing on the OS deformation curves denote the 95% confidence interval. (b.1) Vimentin and keratin fluorescent stain of the WT 3T3 mouse fibroblasts and the vimentin-negative mouse fibroblasts. (b.2) Relative deformation of the mouse fibroblasts cell lines. The 3T3 Vim $-/-$ (in green) show a high active contractility, whereas the Vim $+/+$ (in blue) tend to have a contractile behavior, which is less active than that of the Vim $-/-$. (c) Box plot of the contractile stress for each cell line (listed in order of aggressiveness on the EMT scale) upon optical stretching. Asterisks indicate the level of significance of the two-sided Kolmogorov–Smirnov test with the values $p < 0.05$ (significant), $p < 0.01$ (very significant), $p < 0.001$ (very significant) for one, two and three asterisks, respectively.

chose the epithelial MCF-10A cells, as they are characterized by the densest IF network among the cell lines selected for this study. Cells were seeded in the chip's culture chamber and let migrate through the constrictions upon chemoattractant stimulation. In this case, the micro-funnel was followed by a 40 μm long channel with parallel walls, which prolonged the compressive stress applied on the cells (figure 2(a)). Methanol cell fixation and immunostaining was performed after multiple cells reached the collecting chamber, approximately four days after seeding. By the fourth day, the culture chamber had reached

Table 2. Summary of results.

Cell type	Molecular classification	Invasiveness in microconstrictions	Actin stress fibers formation	Vimentin expression	CK8 expression	CK5 expression	CK6a/6b expression	Active contractility
MCF-10A (EGF-free)	Ba	No	No	Reduced	No	Yes	Yes	Reduced
MCF-10A	Ba	Yes	Yes	Yes	Yes	Yes	Yes	Yes
MCF-7	LA	No	No	No	Yes	No	No	No
MDA-MB-468	TNA	Yes	Yes	No	Yes	Yes	Yes	Yes
MDA-MB-436	TNA	No	No	Yes	Yes	Yes	No	No
MDA-MB-231	TNB	Yes	Yes	Yes	Yes	Yes	No	Yes
MF Vim −/−	Fibroblasts	Yes	Yes	No	No	No	No	Yes
MF Vim +/+	Fibroblasts	Yes	Yes	Yes	No	No	No	Yes

approximately 70% confluence which caused some cells to form cell–cell contacts with their neighbors and migrate collectively toward the micro-constriction row, while other cells where migrating individually. Although the presence of the constrictions constitutes a temporary rupture of this confluent state, cells retained some cell–cell adhesive junctions when reaching the culture chamber (figure 2(b.1)). What we could conclude by observing the cells that have migrated through the narrow channels, is that the filaments arranged into tight bundles while squeezing through, supposedly because of a mere geometric effect imposed by the shape of the constrictions, and temporarily retained a bundled configuration oriented along the direction of migration once they entered the collecting chamber (figure 2(b.1)). In a previous study we observed how migration through the micro-constriction had induced profound alterations in the actin cytoskeleton scaffold, and how cells were unable to rebuild actin stress fibers in the 48 h after squeezing through (Ficorella *et al* 2019). Here, the IFs appear to regain their original configuration relatively fast (within the first 24 h after crossing the constrictions), extending homogeneously from the nucleus to the cells membrane (figure 2(b.2)).

3.2. Cortical contractility bestows invasive aptitude to individually migrating cancer cells

Since vimentin positive mesenchymal cells (MDA-MB-436 and EGF-free MCF-10A) did not display invasive behavior in the microchips, while some vimentin negative cells (MDA-MB-468 and 3T3 NIH Swiss mouse fibroblasts) did, vimentin protein expression does not seem to strongly correlate to the invasive behavior displayed by single cells when migrating through high physical confinement. We then asked whether on a mechanical level a factor exists that can determine which cells can actively navigate through highly compressive spaces, and that at the same time is independent of their tumor phenotype and IF protein expression. A parameter that needs to be considered is the ability of individual cells to deform their shape when squeezing through the constrictions. Cell shape is mainly determined by a stable network of actin filaments, myosin motors and a number of other actin-binding proteins, known as cell cortex. Because the cortex is attached to the cell membrane, its contractions and relaxation play a crucial role in determining cell shape. While fibers-driven contractile forces may originate from polymerization processes such as actin treadmilling (Blanchoin *et al* 2014, Mogilner and Oster 2003, Pellegrin and Mellor 2007, Ridley *et al* 2003), contractile forces that are independent of focal adhesions can be caused by depolymerization and myosin motors activity (Blanchoin *et al* 2014, Gyger *et al* 2014). As we know that actin bundles depolymerization occurs within cells crawling through the micro-constrictions, we asked whether contractility of the actin cortical layer could be the missing element that would explain why certain cell lines, rather than others, show invasive behavior in our setup.

To test this hypothesis, we performed OS measurements for each cell line. The microfluidic OS setup allows to obtain an insight on cell contractility that is independent on focal adhesion and other substrate-dependent force generating mechanisms. Cells in suspension are characterized by a spherical morphology and a cortical layer underlying the plasma membrane, with no actin stress fibers within the cell body. The thickness of the actin cortex is the major contributor to the resistance against a deforming stress (Gyger *et al* 2014). Stretching cells in suspended state generates an active contractile reaction of the actomyosin network that can be quantified through an extended mathematical model built on the Kelvin–Voigt model for viscoelastic materials that includes a linear contractile force. Strictly related to the concept of contractility, is that of optical deformability. Optical deformability is defined as the compliance after a given time t, and depends on the viscoelastic nature of cells. The optical deformability curves were obtained by stretching cells at a laser power of 800 mW for $t = 5$ s. The passive viscoelastic reaction of the cytoplasm does not contribute to the contractility, and is therefore not taken into account. Surprisingly, the results revealed that the cell lines that showed substrate-independent contractile behavior, based on the actomyosin cortex and not stress fibers (arched deformability curves), are the same cell lines that successfully achieved migration through the micro-constrictions, whereas those that showed no active

response to the stretching (straight deformability curve) correspond to the ones that failed to exhibit motile behavior in the micro-constriction chip. Particularly, increasing active contractility of the MCF-10A and MCF-10A w/o EGF cells can be clearly observed from the deformation curve in figure 3(a.1). Quantitative analysis revealed that the median value of the contractility is 0.1287 Pa s^{-1} and 0.0826 Pa s^{-1} for the MCF-10A cells and the EGF-free MCF-10A cells respectively (contractility values are given in figure 3(c)). The MCF-7 cell line, on the other hand, showed no active contractile behavior, which indicates a viscous passive response to the pulling stress exerted by the lasers. Accordingly, the contractility value for the MCF-7 cells is a very low 0.000 011 Pa s^{-1}. The MDA-MB-468 and MDA-MB-231 deformability curves show a contractile behavior, which is however noticeably less pronounced than the that of the epithelial cells (MCF-10A and MCF-10A w/o EGF) (figure 3(a.2)). Such reduction in optical deformability suggests a lower structural resistance of the actin cortex, which is consistent with the ability of mesenchymal cells to navigate through the ECM and intravasate into the lymphatic and circulatory system to reach distant tissues and organs. The contractility values are 0.0174 Pa s^{-1} and 0.0032 Pa s^{-1} for MDA-MB-468 and MDA-MB-231 respectively. Similar to the MCF-7 cells, the metastatic mesenchymal MDA-MB-436 cells display passive viscoelastic behavior, with contractility of 0.0013 Pa s^{-1}.

Finally, we obtained deformability curves of the WT mouse fibroblasts, as well as the vimentin knocked out cells. As mentioned previously, both these cell types exhibited high motility in the micro-chips upon stimulation with sodium pyruvate added to the medium in the collecting chamber, and easily squeezed through the micro-constrictions. They are the only keratin-free cell lines utilized in this study, as confirmed by immunofluorescent labeling (figure 3(b.1)). Both OS curves show a deformable behavior, as in the case of the motile breast cancer cell lines. It is interesting to notice that the vimentin knocked out cells display a more pronounced contractile behavior, with a value of 0.0866 Pa s^{-1}, when compared to the vimentin-positive fibroblasts, whose contractility is 0.0025 Pa s^{-1} (figure 3(b.2)).

Table 2 offers a comprehensive summary of all results.

4. Discussion

Although up-regulation of vimentin expression in keratin positive human breast tumor cells seems to strongly correlate with increased motile behavior in 2D *in vitro* migration, it is yet unclear whether vimentin up-regulation alone confers cells the ability to migrate through sub-nuclear sized pores. Similarly, although cytokeratin expression is considered a reliable prognostic marker in tissue histology, it is not known to what extent specific cytokeratin expression affects single cell invasiveness, or whether its role is limited to resist external stresses for the preservation of cellular integrity. Our micro-constriction assay presents a very special case of cancer cell migration in a dense environment, and although it involves a more complex situation than motility assays on a 2D cover slide, it is yet not a conclusive test to predict cancer cell aggressiveness *in vivo*. However, it decisively allowed us to gain a better understanding of the response of both the actin and IF cytoskeleton to mechanical constraints.

The choice to select clinically well-characterized, and yet very diverse, cell lines was motivated by the desire to observe how cell lines arrayed along the whole phase space of the EMT spectrum (from normal epithelial and stationary to mesenchymal and highly invasive) would behave in our micro-constriction setup, and whether recurring, comparable migratory patterns could emerge.

Our analysis of the IF content in the eight cell lines shows that vimentin expression alone may not be a boost to single cell motility and invasion. Our findings show that the vimentin negative cell lines (MDA-MB-468 and mutant 3T3 mouse fibroblasts) were able to squeeze through the narrow channels, whereas vimentin positive mesenchymal cells (MDA-MB-436) were not able to do so. This contradicts the idea that vimentin expression is restricted to cell lines exhibiting high migratory abilities and that the lack of vimentin expression constitutes an impediment to cell motility.

Contrary to what happens during microfilament (MF) and microtubule (MT) de-polymerization, the vimentin network does not completely disassemble into its monomeric units. Rather, its remodeling appears to occur via constant cyclic splitting and re-annealing of small clusters (Danielsson *et al* 2018). Similarly, depolymerization of keratin bundles normally occurs because of dramatic events, such as infections or use of drugs (Zhu *et al* 2013). Labeling the IFs upon migration of MCF-10A cells through the narrow channels have revealed some interesting differences between the general behavior of the keratin/vimentin networks and that of the actin filament network. Our experiments suggest that no depolymerization of IFs occurs when cells crawl through the rigid constrictions, in spite of their narrow cross-sectional area. Some cells exhibited an elongated shape with bundled keratin and vimentin structures, whereas others showed a rounder shape and the typical homogeneous distribution of the IF cytoskeleton. This not only suggests that IFs can easily arrange themselves in a bundled configuration as the cells deform themselves into a morphology dictated by the shape of the constriction; it also indicates that they can regain

their spread-out configuration from the nucleus to the plasma membrane within a relatively short time after undergoing compression (within 24 h).

While rheological studies have shown that semiflexible biopolymer networks such as vimentin soften under compression (Oosten *et al* 2016) and strain stiffen under shear stress (Janmey *et al* 2007), *in vitro* assays on semiflexible biopolymer do not appear to be conclusive when dealing with living animal cells. An objection to the idea of semiflexible biopolymer network compression softening in live cells was provided by Gandikota *et al*, whose atomic force microscope experiments on mouse embryonic fibroblasts have shown that cells do experience compression stiffening when undergoing uniaxial compression (Gandikota *et al* 2019). In our assay, vimentin and keratin filaments appear to behave in the same fashion when cells undergo compression inside the micro-constrictions. The similarity in their behavior can be easily accounted for by the fact that both vimentin and keratin share very similar polymeric properties, such as mechanical stiffness determined by the persistence length, that has been consistently found to lie in a range between a few hundred nm and a few μm by various experimental techniques (Block *et al* 2015). We also find no indication that compression stiffening, if it occurred, plays any role in preventing the motile cell lines to invade through the narrow constrictions.

Since there seems to be no obvious mechanical reason for malignant motile cells to favor the expression of vimentin over keratin, or vice versa, on a single cell level when navigating through sub-nuclear-sized pores, it is legit to assume that cell invasiveness in our assay cannot be deducible by mere IF protein expression. Aside from providing a resilient and semi-flexible scaffold to the cells, keratin IFs may not have as much of a role in single cell motility, as they do in collective cell behavior, given their contribution to strong epithelial cell–cell adhesion complexes through their bond to desmosome intracellular junctions. Similarly, the fact that vimentin expression is linked to increased cell motility may be beneficial to discern between neoplastic and healthy epithelial cells, but it may also not necessarily relate to the ability of an individual cell to invade its surroundings. Overall, the two types of IFs seem limited to a role of structural support to individual cells navigating through the micro-constrictions, while they may earn their role as cancer markers when considered at a multi-cellular level.

We then shifted our attention to another parameter that is known to play a role in cell motility, namely cell contractility. Because actin stress fibers contractility ceases to play a role when single cells enter the constrictions and start squeezing through the narrow aperture (Ficorella *et al* 2019), we focused our attention on acto-myosin driven contractility of the cell cortex. Activity of the actomyosin network allows cells to deform their shape and squeeze through narrow pores by contracting themselves without adhesion to the local ECM. From the OS deformability curves we obtained for each cell lines, we found that cells that can actively migrate through the narrowing constrictions, also have the ability to actively contract, to different degrees, their actin cortex when undergoing laser stretching forces. This suggests not only that cells can easily switch between different contractility mechanisms during invasion, depending on the nature of their micro-environment; but also that, from a mechanical perspective, invasive ability is also bestowed to cells through contractility, since cells that can generate more force and actively contract when subject to external stresses will have an advantage in situations of high confinement.

The EGF-free MCF-10A cells displayed contractile behavior but lower optical deformability (higher stiffness) than the original MCF-10A cells, which may account for the reduced motility and arrest of motion of the monolayer after reaching the micro-constriction row. Growing the MCF-10A cells in EGF-free medium appear to have caused important alterations in the expression of their cytoplasmic protein. Immunofluorescence revealed downregulation of vimentin and likely downregulation of keratin proteins, whereas western blots confirmed absence of luminal CK8. However, we cannot conclude that the reduced migratory ability of the EGF-free cells is the consequence of vimentin downregulation alone. It is legit to assume that the real cause is the interplay of numerous factors that emerged from non-exposure to EGF, ranging from protein expression alterations at the molecular level, to increased mechanical stiffness and other unknown molecular changes.

The mesenchymal cell lines that showed invasive ability in the micro-chip (MDA-MB-468 and MDA-MB-231), also showed cortical contractility, which was however noticeably less pronounced than that of the epithelial MCF-10A cells. This is in line with the general idea that epithelial cells are by nature more contractile, with respect to substrate-independent cortical contractility, than mesenchymal cells, which mostly display a stress fiber based substrate-dependent contractility. This also agrees with the fact that reduced resistance to deformation of the actin cortex is required for migration of mesenchymal cells through dense tissues.

Overall, our findings suggest that a cell's invasive ability is not entirely predictable from its tumor phenotype and EMT status. A well-distinct type of contractility that is substrate independent and driven by

the cortical actomyosin machinery, not by stress fibers, could be an important factor to distinguish invasive single carcinoma cells from non-invasive cells, independently of their tumor phenotype.

Acknowledgments

We thank the Magin Lab for providing the Vim+/+ and Vim−/− mouse fibroblasts and the antibodies for the western blots, and in particular Miriam Richter for her advice and supervision of the western blot assays. We also thank Enrico Warmt for the fruitful discussions on cellular contractility. This work is supported by the DFG Grant INST 268/296-1 FUGG, and by the ERC Advanced Grant No. 741350 (HoldCancerBack). The authors declare no competing financial interests.

Data availability statement

The data that support the findings of this study are available upon reasonable request from the authors.

Authors contribution

JAK and RO designed research; CF performed the migration experiments in the micro-constrictions, the fluorescence assays and the western blot assays; HE performed the OS measurements and analyzed the data; FS and RMV fabricated the chips; CF wrote the paper.

ORCID iDs

Carlotta Ficorella https://orcid.org/0000-0001-8012-4289
Rebeca Martínez Vázquez https://orcid.org/0000-0001-8728-5819
Josef A Käs https://orcid.org/0000-0003-3158-2480

References

Blanchoin L, Boujemaa-Paterski R, Sykes C and Plastino J 2014 Actin dynamics, architecture, and mechanics in cell motility *Physiol. Rev.* **94** 235–63

Block J, Schroeder V, Pawelzyk P, Willenbacher N and Köster S 2015 Physical properties of cytoplasmic intermediate filaments *Biochim. Biophys. Acta, Mol. Cell Res.* **1853** 3053–64

Bodnar R J 2013 Epidermal growth factor and epidermal growth factor receptor: the yin and yang in the treatment of cutaneous wounds and cancer *Adv. Wound Care* **2** 24–9

Chiang A C and Massagué J 2008 Molecular basis of metastasis *New Engl. J. Med.* **359** 2814–23

Chugh P and Paluch E K 2018 The actin cortex at a glance *J. Cell Sci.* **131** jcs186254

Danielsson F, Peterson M K, Araújo H C, Lautenschläger F and Gad A K B 2018 Vimentin diversity in health and disease *Cells* **7** 147

Domagala W, Lasota J, Bartkowiak J, Weber K and Osborn M 1990 Vimentin is preferentially expressed in human breast carcinomas with low estrogen receptor and high Ki-67 growth fraction *Am. J. Pathol.* **136** 219–27 PMID: 2153347

Ficorella C, Vázquez R M, Heine P, Lepera E, Cao J, Warmt E, Osellame R and Käs J A 2019 Normal epithelial and triple-negative breast cancer cells show the same invasion potential in rigid spatial confinement *New J. Phys.* **21** 083016

Gandikota M C, Pogoda K, van Oosten A, Engstrom T A, Patteson A E, Janmey P A and Schwarz J M 2019 Loops versus lines and the compression stiffening of cells (arXiv:1908.03725)

Gardel M L, Kasza K E, Brangwynne C P, Liu J and Weitz D A 2008 Chapter 19 mechanical response of cytoskeletal networks *Methods Cell. Biol.* **89** 487–519

Gardel M L, Schneider I C, Aratyn-Schaus Y and Waterman C M 2010 Mechanical integration of actin and adhesion dynamics in cell migration *Annu. Rev. Cell Dev. Biol.* **26** 315–33

Guck J, Ananthakrishnan R, Mahmood H, Moon T J, Cunningham C C and Käs J 2001 The optical stretcher: a novel laser tool to micromanipulate cells *Biophys. J.* **81** 767–84

Guck J *et al* 2005 Optical deformability as an inherent cell marker for testing malignant transformation and metastatic competence *Biophys. J.* **88** 3689–98

Gyger M, Stange R, Kießling T R, Fritsch A, Kostelnik K B, Beck-Sickinger A G, Zink M and Käs J A 2014 Active contractions in single suspended epithelial cells *Eur. Biophys. J.* **43** 11–23

Hendrix M J, Seftor E A, Seftor R E and Trevor K T 1997 Experimental co-expression of vimentin and keratin intermediate filaments in human breast cancer cells results in phenotypic interconversion and increased invasive behavior *Am. J. Pathol.* **150** 483–95 PMID: 9033265

Hu J *et al* 2019 High stretchability, strength, and toughness of living cells enabled by hyperelastic vimentin intermediate filaments *Proc. Natl Acad. Sci. USA* **116** 17175–80

Ilina O *et al* 2020 Cell–cell adhesion and 3D matrix confinement determine jamming transitions in breast cancer invasion *Nat. Cell Biol.* **22** 1103–15

Janmey P A, McCormick M E, Rammensee S, Leight J L, Georges P C and MacKintosh F C 2007 Negative normal stress in semiflexible biopolymer gels *Nat. Mater.* **6** 48–51

Kalluri R and Weinberg R A 2009 The basics of epithelial-mesenchymal transition *J. Clin. Invest.* **119** 1420–8

Karantza V 2011 Keratins in health and cancer: more than mere epithelial cell markers *Oncogene* **30** 127–38

Kokkinos M I, Wafai R, Wong M K, Newgreen D F, Thompson E W and Waltham M 2007 Vimentin and epithelial-mesenchymal transition in human breast cancer—observations *in vitro* and *in vivo Cells Tissues Organs* **185** 191–203
Kraning-Rush C M, Califano J P and Reinhart-King C A 2012 Cellular traction stresses increase with increasing metastatic potential *PloS One* **7** e32572
Ku N-O, Toivola D M, Strnad P and Omary M B 2010 Cytoskeletal keratin glycosylation protects epithelial tissue from injury *Nat. Cell Biol.* **12** 876–85
Lange J R and Fabry B 2013 Cell and tissue mechanics in cell migration *Exp. Cell Res.* **319** 2418–23
Mendez M G, Kojima S I and Goldman R D 2010 Vimentin induces changes in cell shape, motility, and adhesion during the epithelial to mesenchymal transition *FASEB J.* **24** 1838–51
Mierke C T 2015 Physical view on the interactions between cancer cells and the endothelial cell lining during cancer cell transmigration and invasion *Biophys. Rev. Lett.* **10** 1–24
Mierke C T, Rösel D, Fabry B and Brábek J 2008 Contractile forces in tumor cell migration *Eur. J. Cell Biol.* **87** 669–76
Mogilner A and Oster G 2003 Force generation by actin polymerization II: the elastic ratchet and tethered filaments *Biophys. J.* **84** 1591–605
Moll R, Divo M and Langbein L 2008 The human keratins: biology and pathology *Histochem. Cell Biol.* **129** 705–33
Moriya T, Kozuka Y, Kanomata N, Tse G M and Tan P-H 2009 The role of immunohistochemistry in the differential diagnosis of breast lesions *Pathology* **41** 68–76
Murrell M, Oakes P W, Lenz M and Gardel M L 2015 Forcing cells into shape: the mechanics of actomyosin contractility *Nat. Rev. Mol. Cell Biol.* **16** 486–98
van Oosten A S G, Vahabi M, Licup A J, Sharma A, Galie P A, MacKintosh F C and Janmey P A 2016 Uncoupling shear and uniaxial elastic moduli of semiflexible biopolymer networks: compression-softening and stretch-stiffening *Sci. Rep.* **6** 19270
Patteson A E *et al* 2019 Vimentin protects cells against nuclear rupture and DNA damage during migration *J. Cell Biol.* **218** 4079–92
Pellegrin S and Mellor H 2007 Actin stress fibres *J. Cell Sci.* **120** 3491–9
Polioudaki H, Agelaki S, Chiotaki R, Politaki E, Mavroudis D, Matikas A, Georgoulias V and Theodoropoulos P A 2015 Variable expression levels of keratin and vimentin reveal differential EMT status of circulating tumor cells and correlation with clinical characteristics and outcome of patients with metastatic breast cancer *BMC Cancer* **15** 399
Qu Y, Han B, Yu Y, Yao W, Bose S, Karlan B Y, Giuliano A E and Cui X 2015 Evaluation of MCF10A as a reliable model for normal human mammary epithelial cells *PLoS One* **10** e0131285
Raymond W A and Leong A S-Y 1989 Vimentin-a new prognostic parameter in breast carcinoma? *J. Pathol.* **158** 107–14
Ribatti D, Tamma R and Annese T 2020 Epithelial-mesenchymal transition in cancer: a historical overview *Transl. Oncol.* **13** 100773
Ridley A J, Schwartz M A, Burridge K, Firtel R A, Ginsberg M H, Borisy G, Parsons J T and Horwitz A R 2003 Cell migration: integrating signals from front to back *Science* **302** 1704–9
Sala F, Ficorella C, Martínez Vázquez R, Eichholz H M, Käs J A and Osellame R 2021 Rapid prototyping of 3D biochips for cell motility studies using two-photon polymerization *Front. Bioeng. Biotechnol.* **9** 664094
Salbreux G, Charras G and Paluch E 2012 Actin cortex mechanics and cellular morphogenesis *Trends Cell Biol.* **22** 536–45
Seltmann K, Fritsch A W, Käs J A and Magin T M 2013 Keratins significantly contribute to cell stiffness and impact invasive behavior *Proc. Natl Acad. Sci.* **110** 18507–12
Shao M-M, Chan S K, Yu A M C, Lam C C F, Tsang J Y S, Lui P C W, Law B K B, Tan P-H and Tse G M 2012 Keratin expression in breast cancers *Virchows Arch.* **461** 313–22
Thompson E W *et al* 1992 Association of increased basement membrane invasiveness with absence of estrogen receptor and expression of vimentin in human breast cancer cell lines *J. Cell. Physiol.* **150** 534–44
Weng Y-R, Cui Y and Fang J-Y 2012 Biological functions of cytokeratin 18 in cancer *Mol. Cancer Res.* **10** 485–93
Wong R W C and Guillaud L 2004 The role of epidermal growth factor and its receptors in mammalian CNS *Cytokine Growth Factor Rev.* **15** 147–56
Wullkopf L, West A-K V, Leijnse N, Cox T R, Madsen C D, Oddershede L B and Erler J T 2018 Cancer cells' ability to mechanically adjust to extracellular matrix stiffness correlates with their invasive potential *Mol. Biol. Cell* **29** 2378–85
Zhu C, Bai Y, Liu Q, Li D, Hong J, Yang Z, Cui L, Hua X and Yuan C 2013 Depolymerization of cytokeratin intermediate filaments facilitates intracellular infection of HeLa cells by bartonella henselae *J. Infect. Dis.* **207** 1397–405